The impact of traditional neuroimaging methods on the spatial localization of cortical areas

Timothy S. Coalson[a], David C. Van Essen[a,1], and Matthew F. Glasser[a,b,1]

[a]Department of Neuroscience, Washington University School of Medicine, St. Louis, MO 63110; and [b]St. Luke's Hospital, St. Louis, MO 63017

Localizing human brain functions is a long-standing goal in systems neuroscience. Toward this goal, neuroimaging studies have traditionally used volume-based smoothing, registered data to volume-based standard spaces, and reported results relative to volume-based parcellations. A novel 360-area surface-based cortical parcellation was recently generated using multimodal data from the Human Connectome Project, and a volume-based version of this parcellation has frequently been requested for use with traditional volume-based analyses. However, given the major methodological differences between traditional volumetric and Human Connectome Project-style processing, the utility and interpretability of such an altered parcellation must first be established. By starting from automatically generated individual-subject parcellations and processing them with different methodological approaches, we show that traditional processing steps, especially volume-based smoothing and registration, substantially degrade cortical area localization compared with surface-based approaches. We also show that surface-based registration using features closely tied to cortical areas, rather than to folding patterns alone, improves the alignment of areas, and that the benefits of high-resolution acquisitions are largely unexploited by traditional volume-based methods. Quantitatively, we show that the most common version of the traditional approach has spatial localization that is only 35% as good as the best surface-based method as assessed using two objective measures (peak areal probabilities and "captured area fraction" for maximum probability maps). Finally, we demonstrate that substantial challenges exist when attempting to accurately represent volume-based group analysis results on the surface, which has important implications for the interpretability of studies, both past and future, that use these volume-based methods.

cross-subject alignment | neuroimaging analysis | blurring | CIFTI grayordinates | standard space

Since the 19th century, neuroscientists have tried to relate human behavior to particular functionally specialized regions within the brain. Meaningful correlations between brain function and anatomy were first achieved by postmortem mapping of lesion locations in subjects having specific behavioral deficits in life (reviewed in ref. 1). Neuroanatomists later began subdividing the cerebral cortex into distinct areas based on cytoarchitecture (e.g., ref. 2) and myeloarchitecture (reviewed in ref. 3) with the hope that well-defined brain areas could be assigned specific behavioral functions.

When noninvasive methods for mapping human brain function became available, first with PET (e.g., ref. 4) and then fMRI (e.g., ref. 5), it also became desirable to establish spatial correspondence across individuals and studies using standard stereotactic coordinate spaces, borrowing an idea from neurosurgical practice. Brodmann's parcellation (2) became especially popular in the neuroimaging community, not necessarily because it was the best, but because Talairach and Tournoux demarcated the approximate locations of Brodmann areas in their standard space (6), which was then mapped to the population average Montreal Neurological Institute (MNI) space (7).

An early and still widely used method for assessing statistical significance in functional brain imaging, statistical parametric mapping using Gaussian random-field theory requires volumetric smoothing to satisfy its underlying assumptions (e.g., ref. 8), resulting in the widespread adoption of smoothing in brain-imaging studies. Spatial smoothing has the seductive side effect of increasing the statistical significance of weak effects in small sample sizes, but at the expense of spatial localization precision (9, 10). Traditionally, smoothed group functional activations are then statistically thresholded and summarized by single 3D coordinates that may be assigned Brodmann's areas or gyral and sulcal designations. Unfortunately, these standard coordinates are imprecisely related to the underlying functional neuroanatomy—the cortical areas—whose neuronal populations generate the functional activations under study (9, 10).

Besides the reductions in precision from spatial smoothing and representing brain functional neuroanatomy with single 3D coordinates, another key issue is the approach used for cross-subject alignment. Because of the high degree of individual variability in cortical folding patterns, and in the location of many areal boundaries relative to folds (11, 12), traditional volume-based methods for aligning cortical areas are imprecise across much of the cerebral cortex (9). Progress in characterizing the functions of brain areas has been impeded by these factors, along with the distributed nature of many brain functions and the lack of an accurate map of human cortical areas.

Significance

Most human brain-imaging studies have traditionally used low-resolution images, inaccurate methods of cross-subject alignment, and extensive blurring. Recently, a high-resolution approach with more accurate alignment and minimized blurring was used by the Human Connectome Project to generate a multimodal map of human cortical areas in hundreds of individuals. Starting from these data, we systematically compared these two approaches, showing that the traditional approach is nearly three times worse than the Human Connectome Project's improved approach in two objective measures of spatial localization of cortical areas. Furthermore, we demonstrate considerable challenges in comparing data across the two approaches and, as a result, argue that there is an urgent need for the field to adopt more accurate methods of data acquisition and analysis.

Surface-based approaches enable more precise spatial localization than traditional volume-based approaches (9), and have been in use for some time, particularly in studies of the visual cortex (13–15).

The recently reported HCP-MMP1.0 multimodal cortical parcellation (https://balsa.wustl.edu/study/RVVG) contains 180 distinct areas per hemisphere and was generated from hundreds of healthy young adult subjects from the Human Connectome Project (HCP) using data precisely aligned with the HCP's surface-based neuroimaging analysis approach (16). Each cortical area is defined by multiple features, such as those representing architecture, function, connectivity, or topographic maps of visual space. This multimodal parcellation has generated widespread interest, with many investigators asking how to relate its cortical areas to data processed using the traditional neuroimaging approach. Because volume-registered analysis of the cortex in MNI space is still widely used (17), this has often translated into concrete requests, such as: "Please provide the HCP-MMP1.0 parcellation in standard MNI volume space." Here, we investigate quantitatively the drawbacks of traditional volume-based analyses and document that much of the HCP-MMP1.0 parcellation cannot be faithfully represented when mapped to a traditional volume-based atlas.

There are four key differences between the traditional volume-based neuroimaging approach and the HCP-style approach (for details, see ref. 9): (*i*) Spatial resolution of images: The HCP acquired structural images (T1w and T2w) at 0.7-mm isotropic resolution (higher than the typical 1-mm acquisition) and used FreeSurfer's cortical segmentation algorithms (reviewed in ref. 18) for robust, high-quality cortical surface models (19). For fMRI, the HCP acquired data at 2-mm isotropic resolution, better than the mean cortical thickness [2.6 mm, range 1.6–4 mm (9)], whereas fMRI is traditionally acquired more coarsely (typically 3- to 4-mm isotropic). (*ii*) Distortion correction: The HCP-style approach corrects fMRI data for distortion induced by inhomogeneity in the main (B0) magnetic field using a field map, which is often neglected in the traditional approach, leading to a mismatch between the fMRI and anatomical data. (*iii*) Spatial smoothing: The HCP-style approach keeps spatial smoothing to a minimum, instead averaging within parcels when appropriate to improve statistical sensitivity and power. The traditional approach uses extensive volume-based spatial smoothing to increase statistical significance, satisfy statistical assumptions, and strive to compensate for imperfect cross-subject alignment. (*iv*) Cross-subject alignment: The HCP-style approach gently initializes alignment of cortical areas on the surface using cortical folding patterns and then aligns areas across subjects using "areal features" (cortical myelin content, resting-state networks, and resting-state topographic maps) that are more closely related to areal boundaries than are structural image intensities in the volume (9) or, to a lesser extent, folding patterns on the surface (20, 21). The resulting standard space is a CIFTI "grayordinates" space that contains both cortical surface vertices and subcortical gray matter voxels (19). In contrast, the traditional volume-based approach strives for alignment using linear or nonlinear volume-based registration of structural image intensities to a standard volume space (reviewed in ref. 22). The HCP-style approach of surface-based alignment grew out of earlier methods that used only folding patterns (12, 23–26) and that, together with surface-based smoothing (e.g., ref. 27), represent intermediate approaches sharing several advantages with the HCP-style approach over the traditional volume-based approach.

We use individual-subject cortical parcellations from the HCP-MMP1.0 generated by an automated areal classifier (16) as a "silver standard" (*Discussion* and *SI Appendix, Supplemental Discussion D4*) to illustrate and quantify the impact of key acquisition and analysis choices on the spatial localization of cortical areas. The individual subject parcellations were derived from each subject's multimodal imaging data in a spatially ag-

nostic manner, and we use a validation group of subjects that share no family relationships with the subjects used for parcellation or classifier training.* These steps minimize concerns about possible circularity in our analysis strategy (*Discussion* and *SI Appendix, Supplemental Discussion D1*). Projecting the individual parcellations into volume space using each subject's own surfaces results in a voxel-wise map of each area in each subject, based on that subject's multimodal data. We use these maps to simulate the effects of different analysis strategies on the degree of spatial overlap of cortical areas across subjects and their arrangement in group averages. The degree to which each analysis approach differs from the HCP-style approach serves as a proxy for what would happen to any neuroanatomically organized dataset if analyzed in a similar way (e.g., an fMRI study, a structural MRI study, etc.). We also include intermediate approaches that use surface registration based on folding alone instead of areal features gently initialized by folding, or use substantial smoothing on the cortical surface. Finally, we illustrate the pitfalls of mapping results from traditional volume-analyzed group-average data onto the surface. Overall, we hope that a deeper appreciation of these issues will accelerate the community's migration away from traditional analyses and toward HCP-style analyses.

Results

Comparing Areal-Feature–Based Surface Registration to Traditional Volume Alignment of Cortical Areas: Probabilistic Maps of Cortical Areas.
We used binary regions of interest (ROIs) from the classifier-based individual parcellations (16) of each of the 210 validation subjects to compute probabilistic maps of each cortical area (i.e., cross-subject averages of the 210 individual subject classifications of each area) (*SI Appendix, Supplemental Methods M1*). For the volume-based analyses, individual cortical areas were mapped back to the volume using individual subject surfaces, reversing the process by which the data were originally brought on to the surface (*SI Appendix, Supplemental Methods M2 and M3*). Fig. 1 shows probabilistic maps of five exemplar areas spanning a range of peak probabilities. Each area is shown as localized by areal-feature–based surface registration (MSMAll) (Fig. 1, *Lower, Center*), and as localized by volume-based methods (FNIRT, parasagittal volume slices). One area (3b in Fig. 1) has a peak probability of 0.92 in the volume (orange, red), whereas the other four have volumetric peak probabilities in the range of 0.35–0.7 (blue, yellow). Notably, the peak probabilities of these five areas are all higher on the surface (Fig. 1, *Lower, Center*) (range 0.90–1) than in the volume, indicating that MSMAll nonlinear surface-based registration provides substantially better functional alignment across subjects than does FNIRT nonlinear volume-based registration.

In Fig. 2*A*, the scatterplot shows that surface peak probabilities are almost exclusively higher and have many more areas with peaks at 100% (54 of 360 on the surface versus only 3 in the volume). Peak volume probabilities have a mean of 0.70 and a SD of 0.17, whereas the peak surface probabilities have a much higher mean (0.94) and a lower SD (0.06). Only 5 of the 360 areas (R_AAIC, R_EC, L_AAIC, L_PoI1, and L_MBelt) have a higher peak value in the volume than on the surface (those below the gray line), and for these the differences are very small. Notably, most of these areas are in locations with good folding-based alignment but relatively poor fMRI signal-to-noise ratio (SNR) (which likely reduces the accuracy of MSMAll areal-feature–based alignment).

---

*The only spatial constraint was that the classifiers were applied within searchlights that were large (30 mm in all directions from the group areal definition) relative to the size and variability of cortical area positions in arealfeature–based aligned data. Parcellation regularization steps that occurred after areal classification (dilation, remove islands, and so forth) used only local distance and vertex neighbor information.

NEUROSCIENCE
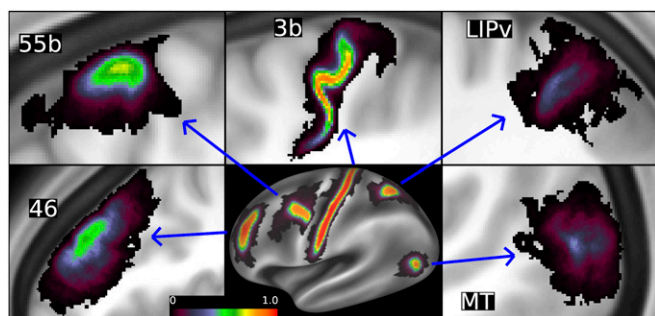
Fig. 1. Probabilistic maps for five areas using both MSMAll areal-feature–based surface registration and FNIRT volume alignment. The volume-based peak probabilities are all lower than the surface-based probabilities for these example areas. Each volume-based area is shown on a parasagittal slice through the peak volumetric probability. See *SI Appendix, Supplemental Methods M2 and M3*. Data are available at https://balsa.wustl.edu/xK0Z.

The peak areal probability only represents information at a single vertex or voxel for each area. To better measure the probabilistic spatial spread of each area, we measured the proportion of each area's vertices or voxels across all individuals that were contained within the group definition of the area, simulating the application of the group parcellation to the data (*SI Appendix, Supplemental Methods M3 and M7*). This measure is derived from the idea that each cortical gray matter area will in some situations generate a distinctive "signal" relative to other areas that is common across individuals (i.e., fMRI timeseries, myelin content, and so forth). We use this concept for evaluating and comparing methods by asking what proportion of the individuals' simulated signal overlaps with (or is "captured" by) the surface-based and volume-based group areal definitions [from the maximum probability map (MPM)] (*SI Appendix, Supplemental Methods M6*). Both the surface-based and volume-based measures use the same per individual volume files to define the simulated signal.

Fig. 2B shows the fraction of the areal signal that lies within the group areal definitions, for both volume and surface. Several different resolutions are simulated, including when the data are acquired with 2-mm voxels (blue dots, simulating data acquired with HCP-style high-resolution fMRI), 0.7-mm voxels (red dots, simulating data acquired at HCP-style structural resolution, such as myelin maps, or ultrahigh-field fMRI), or 4-mm voxels (green

dots, simulating data acquired with "legacy" low-resolution fMRI). In the figure, gray lines connect each area between its 4-, 2-, and 0.7-mm values, revealing how much each method benefits from increases in resolution. This measure is universally higher in MSMAll-aligned surface-based processing than in FNIRT-aligned volume-based processing, with very few areas even approaching equivalence. The median across areas of the surface MPM-captured fraction is 0.56 for simulated 2-mm acquisition resolution, vs. 0.37 for the volume MPM-captured fraction. For simulated 0.7-mm acquisition resolution, the median of the surface-captured fraction increases to 0.67, vs. 0.41 for volume-based methods, suggesting that higher spatial resolution preferentially benefits surface-based analyses. For simulated 4-mm acquisition resolution, the median of the surface-captured fraction is lower (0.43) as expected, but it remains higher than for volume-based methods (0.29), demonstrating benefits of surface-based analyses even for low-resolution, legacy fMRI data [indeed surface-based at 4 mm (0.43) still outperforms volume-based at 0.7 mm (0.41)]. Thus, compared with areal-feature aligned surface-based analyses, an individual's areal signal in volume-based analyses is much more likely to be located outside of the group areal definition. Indeed, on average much less than half of the signal lies inside the group areal definition in volume-based analyses, even before accounting for the smoothing that is traditionally done (see *Effects of Spatial Smoothing in the Volume and on the Surface*, below).

Comparing Areal-Feature–Based Surface Registration to Traditional Volume Alignment of Cortical Areas: Areal Uncertainty. We used binary ROIs of the individual parcellations from each of 210 subjects to compute MPMs for each cortical area and for the noncortical tissue domains ("outside pial" and "inside white") after processing via different approaches (*SI Appendix, Supplemental Methods M1–M3, M6, and M8*). As an objective measure of the quality of spatial alignment, we computed "uncertainty maps," where the uncertainty value equals 1 minus the maximum probability value at each vertex or voxel. Fig. 3 shows the uncertainty measure computed for areal-feature–based surface registration (MSMAll SBR) (Fig. 3A) and for selected parasagittal slices of the FNIRT volume-based registration (FNIRT VBR) (Fig. 3C). The uncertainty values for MSMAll SBR are strikingly lower (better) and more consistent than those for FNIRT VBR. For MSMAll SBR, about half of cortex (49.6%) has uncertainty values less than 0.2 (maximum single area probability >0.8), and only a small percentage of the cortex has
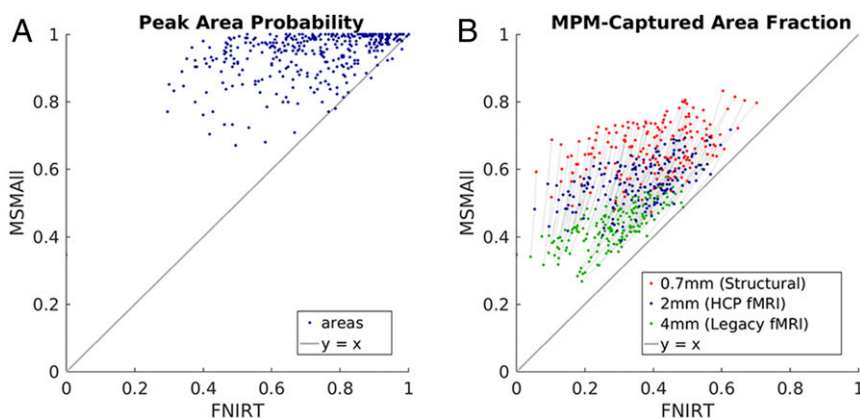
Fig. 2. (A) A scatterplot of areal-feature–based surface registration (MSMAll) peak areal probability vs. volume-based registration (FNIRT) peak areal probability for all 360 areas (180 per hemisphere). (B) A scatterplot of the individual areal signal captured by the group areal definitions (MPMs) (*SI Appendix, Supplemental Methods M6 and M7*) at resolutions of 4-mm functional (e.g., legacy fMRI data, in green), 2-mm functional (e.g., HCP-style fMRI, in blue), and 0.7-mm structural (e.g., myelin or ultrahigh field fMRI, in red). In the right scatter plot, gray lines connect the three data points for each area (averaged across hemispheres, 180 total) showing the degree to which surface-based and volume-based methods benefit from increased resolution (with intermediate resolutions lying along the lines). See *SI Appendix, Supplemental Methods M2, M3, M6, and M7*.
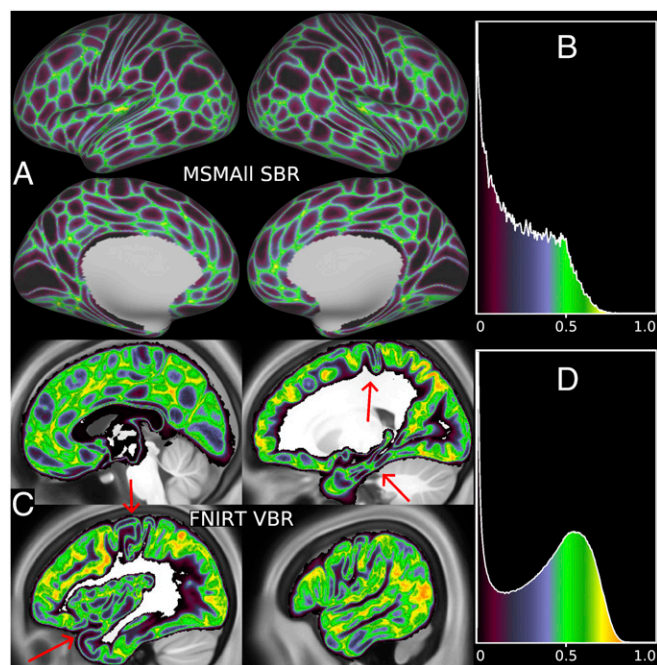
Fig. 3. Areal uncertainty of MSMAll surface-based alignment (*A*) versus FNIRT volume-based alignment (*C*) for the 210V probabilistic cortical areas. The traditional volume-based approach has substantially greater uncertainty (greens, yellows, and oranges) than the HCP-style surface-based approach as seen in the histograms (*B* and *D*) as well as the images (*A* and *C*). In the volume-based results, some locations have low uncertainty (purple and black) and relatively sharp boundaries between areas (red arrows: early sensorimotor, insular, and inferior temporal cortex), comparable to what is consistently found on the surface. The volume ROIs that were used to create this figure were generated by mapping the individuals' parcellations to the 0.7-mm MNI template space using the indiivduals' native resolution MNI space surfaces and the ribbon-mapping method (19). Using 0.7-mm voxels minimizes the effects of voxel size on the group probability maps, allowing the effect of alignment to be investigated separately from the effect of voxel resolution. In practice, typical fMRI resolutions lead to increased signal mixing between areas and noncortical tissues, for both surface and volume analysis (see *Effect of Acquisition Resolution*). See *SI Appendix, Supplemental Methods M2, M3, and M8*. Data are available at https://balsa.wustl.edu/PGX1.

uncertainty values above 0.5 (9.0%). Note that we expect uncertainty to reach 0.5 at boundaries between two areas, and to be even higher at junctions of more than two areas, even if the registration and classification steps had resulted in nearly perfect overlap of areas across subjects. The consistently sharp transition near areal boundaries and the low overall values reflect both the high quality of areal alignment in this registration and the consistency of the parcellation across individuals. Even in regions that are typically challenging to align because of high folding variability (such as the prefrontal cortex) (*SI Appendix,* Fig. S1), uncertainty values near 0.5 are almost entirely confined to narrow strips along the boundaries between cortical areas. The largely uniform and low-valued uncertainty pattern, even in known challenging locations, indicates excellent cross-subject alignment with MSMAll surface registration (see Fig. 6 for a comparison with surface registrations based solely on folding).

In the FNIRT volume-based alignment, some low folding variability locations show reasonably good cross-subject agreement, such as the central sulcus and insula (Fig. 3, red arrows). In these locations the higher uncertainties are locally restricted to obvious boundaries between areas, or between the cortex and the cerebrospinal fluid (CSF) or white matter. However, very little cortex has uncertainty below 0.2 (only 3.3% of the voxels where cortex is the most likely tissue), and almost two-thirds of the cortex has

uncertainty above 0.5 (65.5% of voxels where cortex is the most likely tissue). The higher uncertainty is concentrated in regions of high cortical folding variability (see also *SI Appendix,* Fig. S1). Additionally, the volume-based uncertainty maps contain both uncertainty in gray matter alignment and uncertainty in areal alignment (see also *SI Appendix,* Fig. S2). These high uncertainties show that volume-based registration failed to align the HCP-MMP1.0 areas across subjects in many locations. Notably, most of the very low values in the volume histogram (Fig. 3*D*) are from the wide low-uncertainty fringes that are in atlas white matter and CSF, rather than in locations that are highest probability gray matter (*SI Appendix,* Fig. S3). In contrast, the low values of the surface uncertainty (*SI Appendix,* Fig. S3, *Top Right*) occur exclusively inside gray matter cortical areas. Taken together, these data indicate that FNIRT-based volume analysis is unable to reliably discriminate between cortical areas over much of the neocortex.

Volumetric Areal MPMs. Volumetric MPMs (vMPM) for cortical areas have been reported in other studies (e.g., ref. 28), and we generated volumetric MPMs for the HCP-MMP1.0 parcellation, as described in *SI Appendix, Supplemental Methods M6*. We found that in regions where the probabilistic gray matter ribbon has relatively high values and low areal uncertainties, the vMPM forms a thick continuous ribbon, roughly comparable to average cortical thickness in these regions. In such regions, volume-based alignment is not at a major disadvantage to surface-based alignment. In contrast, for regions where probabilistic cortical gray matter is less well aligned and areal uncertainty is consistently high, the vMPM is thinner than the average cortical thickness. Indeed, in a few locations there are overt gaps that lack a winning cortical area, identifying regions where white matter or CSF is more likely than any single cortical area (see *Left* side of *SI Appendix,* Fig. S4). This contrasts with the accurate alignment of each individual subject's parcellation, mapped to the volume using the subject's surfaces and displayed on the individual's T1w volume, which completely overlaps the map of the individual's gray matter (see *Right* side of *SI Appendix,* Fig. S4). More generally, the volumetric probabilistic maps for the exemplar areas shown in Fig. 1 represent the expected distribution of data generated by these areas in any dataset that has been registered with FNIRT using the HCP's FNIRT configuration without spatial smoothing. The net result is that each area in the vMPM is much smaller than its corresponding probabilistic map, such that a large fraction of each area's group probability (and therefore signal) will fall outside the vMPM parcel. We quantified this effect above in Fig. 2 for MSMAll surface-based registration vs. FNIRT volume-based alignment (see Fig. 8 for additional analysis approaches). This poor alignment of individual subject cortical areas to the group MPM is a fundamental problem for using a volumetric MPM to represent cortical areas. We next demonstrate that this problem is dramatically exacerbated by the spatial smoothing that is commonly used in volume-based studies.

Effects of Spatial Smoothing in the Volume and on the Surface. Smoothing of volumetric data is widely used as a way to reduce voxel-wise noise, increase measures of statistical significance, and satisfy statistical assumptions. It is also often pre-sumed to compensate for imperfect alignment of cortical areas across subjects. Unfortunately, smoothing in the volume mixes data across tissue compartments and across areal boundaries, including non-contiguous areas on opposite banks of gyral and sulcal folds (9). By treating the binary individual-subject parcellations as patches of idealized signal, we can show the effect of smoothing on the purity and extent of areal signal (*SI Appendix, Supplemental Methods M3 and M4*). This effect is visible as a reduction in peak areal probability and an expansion of the volume-based areal probability maps in Fig. 4, which shows three exemplar areas after different smoothing amounts. Area 3b (Fig. 4, *Top* row) has a relatively tight probabilistic distribution without any

NEUROSCIENCE
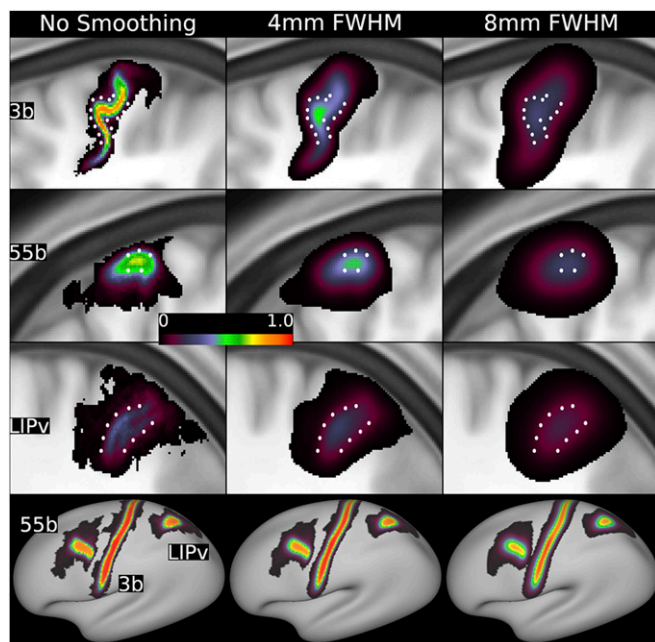
Fig. 4. Effects of volume-based and surface-based smoothing on example cortical areas. The *Top* three rows show enlarged sagittal slices of volumetric probabilistic maps through the maximum probability of three exemplar areas, before (*Left*) and after unconstrained volume-based Gaussian smoothing of 4-mm (*Center*) or 8-mm (*Right*) FWHM. In each row, white dots are in corresponding positions for reference. The *Bottom* row shows the same amounts of surface-based Gaussian smoothing applied to the same three areas after areal-feature–based registration (MSMAll). Areal probability values decrease in the volume after smoothing substantially more than on the surface with the same amount in millimeters FWHM of smoothing. See *SI Appendix, Supplemental Methods M3 and M4*. Data are available at https://balsa.wustl.edu/7Blg.

smoothing (Fig. 4, *Top*, *Left*), but the peak value is markedly reduced and the spatial extent increased with 4-mm full-width half-maximum (FWHM) volumetric smoothing, deleterious trends that worsen with 8-mm FWHM smoothing. Areas 55b and LIPv start out with greater spread in the no-smoothing condition, so the effects of volumetric smoothing are not as visually dramatic, but they are nevertheless substantial in both cases. Comparable levels of surface-based smoothing applied to the same three MSMAll-registered areas (Fig. 4, *Bottom* row) show a much smaller effect, although smoothing still erodes localization.

From the standpoint of cortical localization, volume-based smoothing substantially erodes the fidelity with which areal assignments can be made. This effect is illustrated in the top two rows of Fig. 5, which shows areal uncertainty maps (Fig. 5, second row) and histograms (Fig. 5, *Top* row) without smoothing (Fig. 5, *Left*) and after volumetric smoothing of the group probability maps by 4-mm FWHM (Fig. 5, *Center*) and 8-mm FWHM (Fig. 5, *Right*), which are commonly used levels of volumetric smoothing in fMRI studies. Over most of the cortical ribbon, areal uncertainty in the volume-smoothed maps exceeds 0.5 (green/yellow), especially for 8-mm FWHM smoothing, indicating that neuroanatomical identification at the level of individual cortical areas in the HCP-MMP1.0 parcellation is quite limited indeed. Surface-based smoothing of the areal probability maps at 4- and 8-mm FWHM (Fig. 5, *Lower* rows) also causes some blurring of areal boundaries. However, unlike volume-based smoothing, it does not blur across sulci or across tissue categories, so the overall effects are substantially less deleterious. See *SI Appendix,* Fig. S5 for additional volume smoothing levels of 2-, 6-, and 10-mm FWHM that have been reported for fMRI studies

(17). *SI Appendix,* Fig. S6 shows the additional surface smoothing level of 15-mm FWHM that has been reported in the literature (29) and that approaches the areal uncertainty values seen in un-smoothed volume-based alignment along with the same three levels of smoothing (4, 8, and 15 mm) with a FreeSurfer alignment.

Volume-based smoothing also shifts the location of maximum gray matter probability toward the central CSF-filled portion of sulci and toward the white matter portion of gyri (*SI Appendix,* Fig. S7). Features in regions of low folding variability (e.g., insular cortex and the superior temporal gyrus) are sharply defined without smoothing, as is the boundary between gray and white matter in such regions. With smoothing, the sulcal fundi are not only blurry, but the apparent location of the transition between gray and white matter is substantially shifted, particularly for high smoothing levels (e.g., 8-mm FWHM).

Comparing Areal Alignment Quality of Different Surface-Based Registration Methods. We compared the alignment quality of four different surface-based registration methods (*SI Appendix, Supplemental Methods M4*). Fig. 6 shows results for MSMAll registration (areal-feature–based), MSMSulc (folding–based, with less distortion than FreeSurfer), FreeSurfer (folding–based), and a sphere rotation-only rigid alignment (which has only 3 degrees-of-freedom, whereas spherical warpfields often have thousands) derived from the FreeSurfer registration. Each row in the figure shows surface probabilistic maps for six representative cortical areas, areal uncertainty maps, and histograms of uncertainty values. All three ways of representing the data demonstrate that MSMAll provides the tightest alignment of the HCP-MMP1.0 probabilistic maps (higher peak probabilities and tighter clustering). MSMSulc is intermediate, although only slightly better than FreeSurfer, which in turn is slightly better than spherical rotation overall. The spherical rotation method's alignment is driven
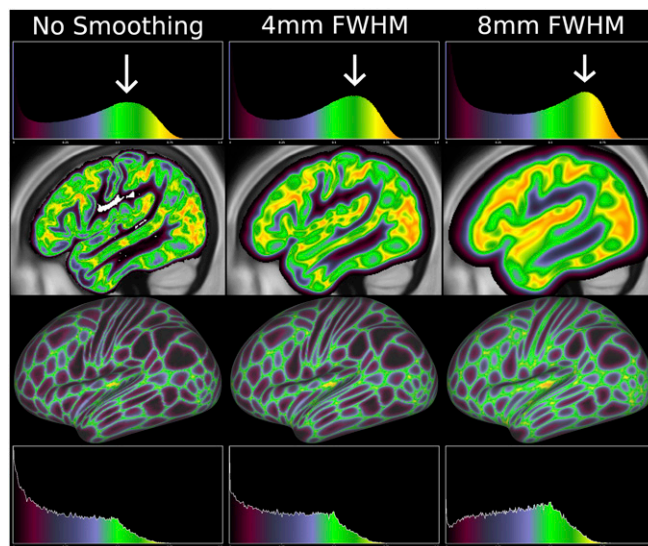
Fig. 5. Comparison of different degrees of smoothing (columns) for both volume-based (*Upper* two rows) and surface-based (*Lower* two rows) approaches. Both areal uncertainty maps and histograms are shown. These were computed by smoothing the probability maps, which is equivalent to smoothing the per subject ROIs before averaging. Smoothing kernels on the surface clearly have less deleterious effects than smoothing kernels of the same size in the volume, because surface smoothing avoids smoothing across sulci or into other tissues. As with Fig. 3, the volume-based histograms have substantial "low uncertainty" tails that arise from poor alignment of the cortical ribbon, and from the tail of the Gaussian smoothing kernel within the white matter and CSF. See *SI Appendix, Supplemental Methods M3, M4, and M8*. Data are available at https://balsa.wustl.edu/6MB7.
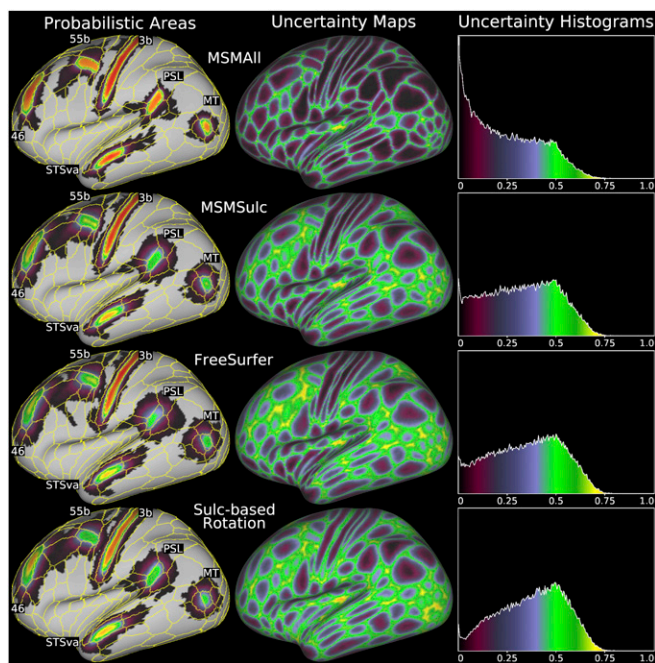
Fig. 6. Comparison of four surface-based alignments: MSMAll areal-feature–based registration (*Top*), MSMSulc folding-based registration (second row), FreeSurfer folding-based registration (third row), and a rigid spherical rotation alignment based on the FreeSurfer registration (*Bottom*). The *Left* column shows six probabilistic areas for each registration approach with yellow contours representing the areal boundaries from the 210V MPM. The *Center* column shows the maps of areal uncertainty (1 minus maximum probability at each vertex), as in Fig. 3. The *Right* column shows the histograms of the uncertainty maps. See *SI Appendix, Supplemental Methods M4*. Data are available at https://balsa.wustl.edu/1616.

primarily by similarities in spherical inflation across subjects. The peak areal probabilities and degree of areal dispersion found here for FreeSurfer folding-based registration is comparable to that reported in previous studies that used FreeSurfer registration with other parcellations (12, 30, 31). Note that the maximum possible overlap on the surface (or in the volume) is less than 100% for some areas because the areal classifier does not detect 100% of all areas in all subjects and because there are atypical topologies in some areas in some subjects that prevent any topology preserving registration from achieving perfect overlap across subjects (*SI Appendix, Supplemental Methods M1*).

Effect of Acquisition Resolution. Of the three main acquisition and analysis choices made in neuroimaging studies that directly impact spatial fidelity (acquisition resolution, method of cross-subject alignment, and method and amount of smoothing), we found that commonly used fMRI acquisition resolution choices have the smallest overall impact (*SI Appendix, Supplemental Methods M2*). Fig. 7 compares how surface-based and volume-based processing is affected by the combination of partial-volume and volume-based tissue alignment effects, at current state-of-the-art 3T fMRI acquisition resolutions (2-mm isotropic) and five other simulated resolutions (0.7–4.0 mm). It shows that partial-volume effects on the surface decrease substantially (gray matter signal fraction increases) when acquiring data with smaller voxel sizes. Notably, for surface-based analysis, the group-average spatial pattern in this measure is largely determined by cortical thickness, and is highly uniform over much of the cortex. In contrast, the histograms of group-average volume data are largely unchanged, despite increases in acquisition resolution, because the inaccuracies of volume-based alignment

largely dominate the measure, showing that traditional volume-based analyses are unable to fully take advantage of higher-resolution data. The maximum volume-based group cortical signal fraction also varies considerably across different regions of the cortex (e.g., between the central sulcus and superior parietal cortex), suggesting spatial heterogeneity in statistical power and localization precision for volume-based analyses.

Although acquisition resolution has the lowest impact among the three aforementioned processing choices, finer acquisition resolution, especially below the mean cortical thickness of 2.6 mm, is very helpful for surface-based studies, which are not limited by volume-based cross-subject alignment. Higher resolutions (e.g., the 1.6-mm voxel size for HCP 7T fMRI data) will reduce partial volume effects and enable more advanced analyses, such as those focusing on laminar differences within the cortical ribbon (9) (*SI Appendix, Fig. S8*). However, such analyses will require technical advances in MRI acquisition, and optimization of trade-offs between voxel size, SNR, and acquisition speed.

Summary Localization Measures for Different Registrations and Smoothing Levels. Fig. 8 provides a valuable summary comparison across a variety of approaches, using the aforementioned peak probability and area capture measures (Fig. 2) for each of the 360 cortical areas. Notably, this figure also includes a new strain-regularized MSMAll surface-based registration (20), which was not used in defining the parcellation or training the areal classifier, but nevertheless shows very similar performance
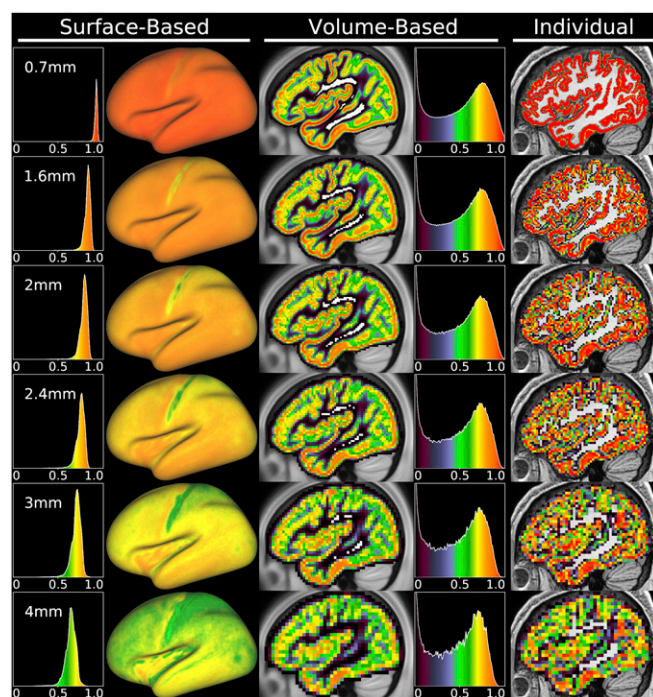
Fig. 7. The effect of acquisition resolution on the separation of cortical signal from noncortical signal, for surface-based (*Left* two columns) and volume-based (*Center* two columns) processing. The measure shown is the group average cortical gray matter fraction of each vertex or voxel. The *Right*-most column shows an individual's (HCP subject 121618) cortical fraction volumes for the same six resolutions, as an example of the inputs to the analyses. Smoothing was not applied. The cortical signal fraction becomes somewhat degraded at the edge of cortex (green voxels) in many regions, even at 2-mm resolution (even though this is less than the mean cortical thickness) and is severely degraded (many green and blue voxels) at traditionally used resolutions between 3 and 4 mm. See *SI Appendix, Supplemental Methods M2*. Data are available at https://balsa.wustl.edu/5gMx.

NEUROSCIENCE
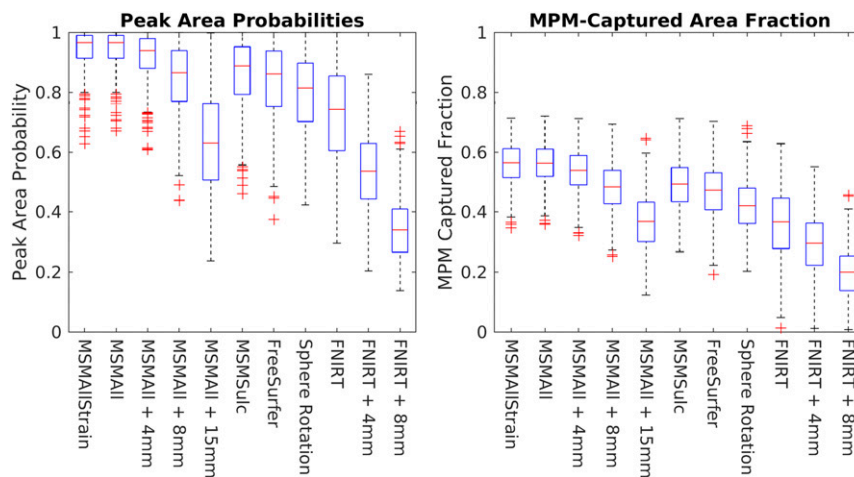
Fig. 8. (*Left*) Box and whisker plots of the peak probability of each area for various SBR methods and for FNIRT volume-based registration, plus the effects of differing amounts of surface (4-, 8-, and 15-mm FWHM) and volume smoothing (4- and 8-mm FWHM). Less optimal registration methods and greater smoothing consistently reduce peak areal probability. Volume-based smoothing has the largest impact, followed by volume-based versus surface-based alignment. The decrease of FreeSurfer compared with MSMSulc is similar in magnitude to that of smoothing MSMAll data by 4-mm FWHM. (*Right*) MPM captured area fraction using 2-mm MNI space voxels for the same 10 methods, showing a similar pattern. Notably, the areas that do worse in the new MSMAllStrain are generally well aligned by folding, whereas the areas that do better in MSMAllStrain have more variability across subjects (the new MSMAllStrain allows more mild-to-moderate distortions while clamping peak distortions). Red line is the median, box edges are the 25–75 percentiles, whiskers are 2.7 SDs, and red pluses are outliers beyond 2.7 SDs. See *SI Appendix, Supplemental Methods M2–M7*.

to the original MSMAll. The *Left* box and whisker plots in Fig. 8 show the peak probabilities of each area, and Fig. 8, *Right* shows the MPM-captured area signal measures for the same 10 methods (using 2-mm resolution partial volume weighting). These measures give the same ranking to the medians of each method, which are tabulated in *SI Appendix*, Table S1. A particularly important comparison shows that the most commonly used smoothing level (17) in the traditional approach (FNIRT + 8-mm FWHM volume smoothing) is only 35% as good as the best surface-based method (MSMAll) using measures of median peak areal probability (0.340 vs. 0.967) and median MPM-captured areal fraction (0.200 vs. 0.564). Comparing the surface-based analysis using only rigid rotation for spherical alignment to the volume-based analysis without smoothing reveals the benefits achieved by simplifying the more challenging cross-subject cortical registration problem from 3D to 2D and solving the more tractable tissue segmentation problem to handle the third dimension. These conceptual improvements reflect the fundamental advantage that surface-based approaches have over volume-based approaches (*SI Appendix, Supplemental Discussion D2*). Large amounts of surface-based smoothing (15-mm FWHM) substantially degrade cortical area localization to levels similar to volume-based alignment with no smoothing.

**Mapping Legacy Group Average Volume Results onto the Surface.** Traditional volume-based analyses often map group-average volume-based results onto group-average surfaces for visualization purposes using, for example, the "average fiducial mapping" approach (24). While this approach has known limitations, its accuracy has not previously been analyzed carefully. We used a modified form of this approach, which we call average surface mapping (ASM), employing the ribbon-based volume to surface mapping technique (19) and the group-average MSMAll white and pial surfaces (*SI Appendix, Supplemental Methods M9*). In *SI Appendix*, Fig. S9 we illustrate the primary pitfall of this approach: group-average surface contours do not consistently follow the group-average cortical ribbon, particularly in regions of high folding variability (see *SI Appendix*, Fig. S9 *B, 2*). Even when using folding-based surface registration, topologically incompatible folding patterns (e.g., two gyri in some subjects where

there typically is only one) lead to reductions in group-average cortical surface area that "shrink" the surface toward the direction of folding, as these patterns are unable to be aligned and therefore result in significant cross-subject variability of coordinates. The folding detail of the group-average surface is further reduced when using average surfaces from MSMAll-registered data instead of folding-based alignment because of discrepancies between function and folds (*SI Appendix*, Fig. S1). Indeed, the MSMAll group-average surfaces only show significant folding detail in locations that have good correspondence between folds and areas. Thus, mapping group-average volume data onto group-average surfaces will have additional biases (on top of the blurring effects from misalignment and smoothing and the biasing effects of smoothing folded cortex shown in *SI Appendix*, Fig. S7). Folding-based average surfaces will be only modestly better that MSMAll surfaces overall.

An alternative approach for mapping group-average volume data to surfaces is the "multifiducial mapping" method, using anatomical midthickness (fiducial) surfaces from many individuals as intermediates (24). Here we similarly modified this method by using ribbon mapping and call this "multiple individual mapping" (MIM). The cortical gray matter fraction map from this approach is smoother, showing less sensitivity to folding patterns, but also has a lower overall value, as shown in *SI Appendix*, Fig. S9 (see *SI Appendix*, Fig. S9 figure legend and *SI Appendix, Supplemental Methods M2 and M9*). This effect occurs because the tissue misalignment from FNIRT is applied twice: once in making the volume-based group-average cortical ribbon and again when mapping the group average onto the individuals' surfaces. This method also results in more mixing between tissue classes, decreasing the cortical contribution to the surface-mapped values.

These effects are apparent when looking at cortical areas as well. Indeed, after averaging the 2-mm MNI-space area maps in the volume, mapping this result onto a large set of individual surfaces, and averaging on the surface, the resulting area maps are dramatically changed relative to the surface-based approach of mapping each individual subject's area volumes onto their own surfaces before averaging (*SI Appendix*, Fig. S10). These effects extend to the maximum partial volume maps as well (Fig. 9). In regions with high folding variability, it is challenging for cortical
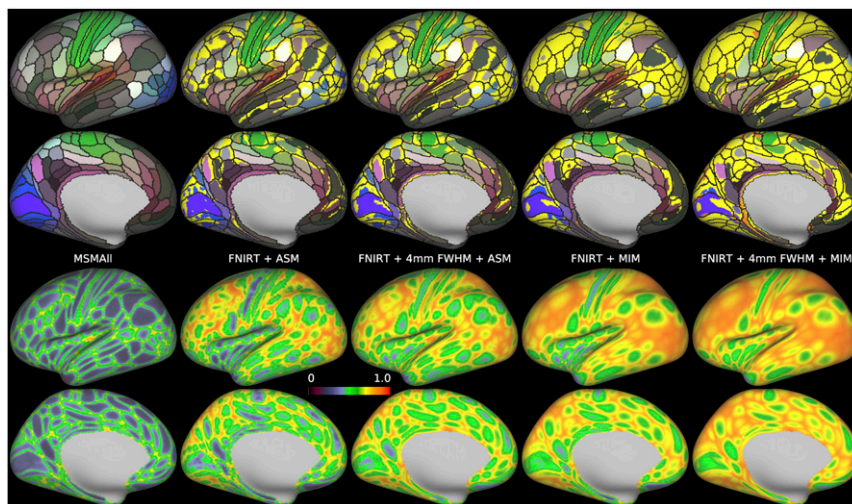
Fig. 9. Comparison of the surface-based maximum partial-volume map to the maps produced after volume-based analysis with ASM or MIM, and 4-mm FWHM volume-based smoothing before ASM and MIM. The figure uses the same methods as *SI Appendix*, Fig. S10, and then uses the maximum fraction to label the surface vertices. In the *Upper* two rows, bright yellow is the white matter label, and bright orange is the CSF label (occurring in only a few small patches). Substantial regions of the cortex are not separated into cortical areas after volume-based analysis and MIM, and ASM shows significant stripes where the gyral crowns are decapitated. On the other hand, in regions of lower folding variability and variability of areas vs. folds, such as the insula, volume-based methods reproduce the parcellation found with the surface-based approach, particularly if smoothing is not used. See *SI Appendix, Supplemental Methods M2 and M9*. Data are available at https://balsa.wustl.edu/nKvx.

areas to be dominant over noncortical tissue classes (white matter in particular), as shown by the extensive bright yellow regions in the top two rows for FNIRT + ASM mapping (Fig. 9, column 2) and their even greater extent for FNIRT + MIM (Fig. 9, column 4). These effects are further exacerbated by volume-based smoothing (Fig. 9, columns 3 and 5). Notably, for some cortical areas that are well aligned by folds, such as those in the insula, the methods are essentially identical across unsmoothed approaches (although again, volume-based smoothing is universally deleterious). However, when analyzing all of the cortex, it is much better to map individual data onto individual surfaces and align the data on the surface if one wants to relate it to surface-based data, including the HCP's multimodal parcellation.

Discussion

We have systematically explored the impact on spatial localization of different acquisition and analysis choices, using a large dataset in which the cerebral neocortex was individually parcellated using multiple modalities. These data allowed us to incisively and quantitatively assess the impact of these methodological choices on spatial localization, not only for the HCP-MMP1.0 parcellation data but also by extension for a wide range of neuroimaging studies (both past and future). The analysis in Fig. 8 summarizes the key results and illustrates the magnitudes of the effects on spatial localization of different analysis choices. Areal-feature–based surface registration (MSMAll or MSMAll-Strain) without smoothing clearly achieves the best localization of the HCP-MMP1.0 areas. The effect of 4-mm FWHM surface-based smoothing on MSMAll-registered data are comparable to the difference between MSMSulc and FreeSurfer folding-based registrations: modest, but still meaningful. The difference between registrations based on areal features vs. folding is comparable to the difference between folding-based surface registration and FNIRT volume-based registration, and also similar to the difference between unsmoothed areal-feature–based surface registration and more heavily smoothed areal-feature–based surface registration at 8-mm FWHM. At 15-mm FWHM surface-based smoothing more substantially degrades MSMAll-aligned cortical areal spatial localization to a level similar to that of unsmoothed FNIRT volume-based alignment. The degradation of spatial lo-

calization from moderate (4-mm FWHM) unconstrained volume-based smoothing is similar to the difference between unsmoothed volume-based registration vs. areal-feature–based registration, and the degradation is substantially greater for the more commonly used 8-mm FWHM volume-based smoothing (17). Importantly, these effects are cumulative, and one cannot "recover" any spatial localization that was lost in previous steps (i.e., smoothing does not ameliorate reductions in spatial localization from registration methods that do not align areas; it instead makes them worse).

Studies that use extensive smoothing typically do not overtly justify their chosen amount of smoothing. The most common smoothing level in the literature is 8-mm FWHM, the default value in SPM, the most commonly used neuroimaging software package (17). While spatial smoothing is indeed effective in increasing statistical sensitivity, so too is improving areal alignment across subjects with surface-based, areal-feature–based registration. Aligning "like with like" tends to improve z-statistics by reducing cross-subject variability (see ref. 9), and it also makes the resulting group maps sharper and more neuroanatomically interpretable rather than making them blurrier and less interpretable, as smoothing does. Use of areal-feature–based registration together with minimal smoothing was critical for creating HCP's multimodal parcellation at the group level (16). Permutation-based nonparametric statistical methods [such as those offered in the PALM software, https://fsl.fmrib.ox.ac.uk/fsl/fslwiki/PALM (32)] can be used without smoothing, or with small amounts of smoothing, in contrast to popular parametric methods, and also work well with HCP-style CIFTI or parcellated data. The statistical assumptions required by Gaussian random-field theory, which have been assumed to be satisfied by using large smoothing kernels, were recently shown to be unsatisfied in some cases, leading to increased false positives (33).

Surface-based representations of cortical data are more visually informative than volume-based depictions, insofar as the convoluted sheet-like cerebral cortex is best inspected on a 2D visual model, often using inflation or flattening to expose cortex that is buried inside sulci. Modest surface-based smoothing (e.g., 4-mm FWHM) can increase statistical sensitivity and make maps more visually appealing at the cost of a modest decrease in spatial resolution (e.g., reducing the discriminability of thin features, such as

NEUROSCIENCE

area 3a, or fine details, such as somatotopic variations in myelin content in areas 4 or 3b). Parcellation provides a more powerful alternative to spatial smoothing for increasing statistical sensitivity (16). Parcel-constrained averaging can be considered a neuro-anatomically informed method of smoothing (averaging within cortical areas defined using multiple modalities) that also greatly reduces the number of statistical comparisons.[†] Rather than improving alignment, spatial smoothing further erodes the ability to localize brain structure, function, or connectivity in neuroimaging studies. The statistical sensitivity benefits of spatial smoothing come from reducing the effects of unstructured noise in the data and real cross-subject variability, not from alignment improvements. Notably, other fields concerned with image analysis generally strive to reduce rather than increase blurring of their images (e.g., astronomy uses space telescopes and advanced adaptive optics to counteract the blurring effects of the earth's atmosphere). Additionally, the use of statistical thresholds [which are less reproducible than effect-size maps and spatial gradients (9)], and the tendency to summarize activation clusters as single 3D coordinates induce further spatial localization uncertainty in the traditional volume-based literature. Taken together, these limitations make accurate comparisons between the traditional neuroimaging literature and the HCP's multimodal parcellation very challenging indeed.

Our findings are also unlikely to be the result of circularity (i.e., that MSMAll was intrinsically favored because it had been used in generating the HCP-MMP1.0 parcellation used here to evaluate different acquisition and analysis methods) for the reasons discussed in *SI Appendix, Supplemental Discussion D1*. Briefly, we used a spatially agnostic classifier, analyzed an independent dataset, and replicated the findings with a different version of the registration algorithm that produces a nonidentical solution. Indeed any circularity concerns would be limited to the improvements of MSMAll over and above MSMSulc, which accounts for only ~25% of the threefold improvement of MSMAll over FNIRT with 8-mm smoothing (~50% is related to not doing the smoothing and another ~25% to surface instead of volume alignment). MSMAll has previously been shown to provide major improvements in independent task fMRI data that were not used in the registration (20, 21) over MSMSulc. Thus, we believe any circularity effect is small, if it exists at all, and even in a worst case it would not affect our main conclusions.

Our analysis focused on FMRIB Software Library's (FSL) FNIRT algorithm and alignment to the MNI152 FNIRT nonlinear atlas template because that is how the HCP data were aligned volumetrically. Numerous other algorithms for volumetric alignment are available, and numerous template volumes are used as targets for registration to an atlas. However, we believe that no volume-based registration algorithm that enforces smoothly varying and anatomically plausible amounts of distortion will have better cortical alignment performance than the areal-feature–based surface registration algorithm shown here, even if areal features were used in the volume.[‡] Volume-based registration of incompatible folding patterns and of in-compatible relationships between areas and folds is a profoundly more challenging problem. Surface-based registration achieves a correspondence in 2D on a sphere, which allows spherical registration deformations to ignore incompatible or misleading folding patterns and therefore is unable to mix cortex with white matter or CSF. In contrast, nonlinear volumetric registration is instead defined in terms of anatomical deformations, and must explicitly deal with fundamental folding issues, like two gyri in some subjects where most have only one (see *SI Appendix, Supplemental Discussion D2* for further discussion of alternative volume-based registrations and the fundamental differences between surface and volume-based registration).

On the other hand, even better correspondence across subjects than the current areal-feature–based surface registration may be attainable using improved algorithms within the MSM framework (20), increasing the amount of allowed distortion, or other topology-preserving approaches (e.g., ref. 40). Methods that do not enforce topology preservation, such as individual subject parcellation (16, 41, 42) or hyperalignment (34, 43) can perform even better. Surface based studies, such as those that have used FreeSurfer alignment to the "fsaverage" atlas, can be profitably compared with the HCP-MMP1.0 parcellation (*SI Appendix, Supplemental Discussion D3*). Indeed they are approximately three-quarters of the way toward an HCP-style analysis (Fig. 8). Legacy volume-based studies could be reanalyzed using surface-based methods for accurate comparison with modern maps of the cerebral cortex (e.g., using tools such as CIFTIFY that are expressly designed for this purpose; https://github.com/edickie/ciftify). Finally, it is worth remembering that while we believe the HCP's MMP1.0 is the best available map of human cerebral cortical areas, we expect future refinements as more data become available and more investigators tackle the cortical parcellation problem using semiautomated, HCP-style approaches (*SI Appendix, Supplemental Discussion D4*).

Concluding Remarks

For decades, human neuroimaging studies have been dominated by an analysis paradigm consisting of volumetric alignment of cortical data coupled with unconstrained volumetric spatial smoothing. Unfortunately, this volumetric alignment is inaccurate for most of human neocortex, and results in statistically significant blobs whose precise relationship to cortical areas is uncertain. These blobs are then represented as 3D volumetric coordinates and assigned to Brodmann areas and coarse folding-related landmarks. Such results generally lack a close resemblance to the fine-grained mosaic of areas that populate the cortical sheet and generate the functional signals measured by these studies (9). Cortical surface-based approaches provide powerful alternatives that have gained momentum since their introduction two decades ago, especially for studies of the visual cortex (e.g., ref. 13), but widespread adoption of surface-based approaches has been slow (9, 26), hampering progress in understanding cortical areas outside the visual system. Factors contributing to this unfortunate situation include: the desire to replicate or compare with existing studies that used the traditional volume-based approach; the relative lack of "turn-key" tools for running a surface-based analysis (but see ref. 19); the learning curve for adopting surface-based analysis methods; unawareness of the problems with traditional volume-based analysis; and uncertainty or even skepticism as to how much of a difference these methodological choices make.

The present study speaks mainly to the last two points, as we have used the HCP's multimodal parcellation to quantify the benefits of aligning data on surfaces instead of in volumes, using areal features instead of folds for this alignment, and minimizing spatial smoothing. These choices have a large impact on spatial localization. Moreover, analysis software and preprocessing pipelines for using "grayordinate-based" analysis and visualization

---

[†]Parcel-based averaging is appropriate for many analyses, but of course not for all. For example, studies of fine-scale cortical topography (e.g., refs. 34–36) depend on preservation of small spatial details and are best analyzed using minimally smoothed data. However, neurobiological interpretation of topographic gradients can benefit from relating the gradients to nearby cortical areas.

[‡]That said, we feel volumetric registration of subcortical structures remains important (for example, the HCP uses the FNIRT nonlinear registration algorithm for subcortical alignment). Furthermore, the use of fiber orientation information may improve white matter fiber-tract alignment in the same way that areal features improve cortical areal alignment (37, 38). Additionally, the use of gentler volume registration algorithms optimized to maximize functional alignment would be beneficial (*SI Appendix*, Figs. S11 and S12), together with including surface-based constraints, which may also help resolve some ambiguities in the volume (39).

are now freely available, such as the HCP pipelines available on github (https://github.com/Washington-University/Pipelines), Connectome Workbench, growing support in FSL, and tools such as CIFTIFY for processing legacy data (https://github.com/edickie/ciftify). FreeSurfer has also provided its own surface-based analysis streams for nearly two decades (18). We hope that these approaches will receive increasing support and adoption in other tools, such as AFNI (SUMA), BrainVoyager, and SPM (CAT).

Rather than continuing with "business as usual" using the traditional volume-based approach, we encourage neuroimaging investigators to reevaluate the methods that they are using. An overreliance on measures of statistical significance to assess scientific validity of brain-imaging studies and an underappreciation of neuroanatomical fundamentals has contributed to recent controversies in neuroimaging (e.g., ref. 33). The issues considered in this and preceding papers (9) are arguably even more problematic, given the vast resources poured into tens of thousands of neuroimaging studies that have yielded blurry results that would require reanalysis to enable accurate comparisons with the sharper picture that is emerging of the functional and structural organization of the cerebral cortex. The future impact of these legacy studies is significantly limited by the difficulty in accurately comparing them to modern surface-based maps of the human cerebral cortex.

Widespread adoption of approaches to data acquisition, analysis, and visualization that preserve high resolution and enable precise spatial localization is vital for accurately relating brain structure, function, and connectivity to well-defined neuroanatomy. Progress in this direction will benefit from recognition and consideration of these issues by investigators, reviewers, journal editors, and funding agencies alike. Accurate relation of brain-mapping results to brain areas can accelerate progress in understanding how the brain works in health and disease.

1. Geschwind N (1974) Disconnexion syndromes in animals and man. *Selected Papers on Language and the Brain* (Springer, Dordrecht, TheNetherlands), pp 105–236.
2. Brodmann K (1909) *Vergleichende Lokalisationslehre der Grosshirnrinde in ihren Prinzipien dargestellt auf Grund des Zellenbaues* (Johann Ambrosius Barth, Leipzig, Germany).
3. Nieuwenhuys R (2013) The myeloarchitectonic studies on the human cerebral cortex of the Vogt-Vogt school, and their significance for the interpretation of functional neuroimaging data. *Brain Struct Funct* 218:303–352.
4. Petersen SE, Fox PT, Posner MI, Mintun M, Raichle ME (1988) Positron emission tomographic studies of the cortical anatomy of single-word processing. *Nature* 331: 585–589.
5. Belliveau JW, et al. (1991) Functional mapping of the human visual cortex by magnetic resonance imaging. *Science* 254:716–719.
6. Talairach J, Tournoux P (1988) *Coplanar Stereotaxic Atlas of the Human Brain* (Thieme Medical, New York).
7. Evans AC, et al. (1993) 3D statistical neuroanatomical models from 305 MRI volumes. *Nuclear Science Symposium and Medical Imaging Conference*, (1993 IEEE Conference Record, Piscataway, NJ), pp 1813–1817.
8. Worsley KJ, et al. (1996) A unified statistical approach for determining significant signals in images of cerebral activation. *Hum Brain Mapp* 4:58–73.
9. Glasser MF, et al. (2016) The Human Connectome Project's neuroimaging approach. *Nat Neurosci* 19:1175–1187.
10. Turner R, Geyer S (2014) Comparing like with like: The power of knowing where you are. *Brain Connect* 4:547–557.
11. Amunts K, Malikovic A, Mohlberg H, Schormann T, Zilles K (2000) Brodmann's areas 17 and 18 brought into stereotaxic space-where and how variable? *Neuroimage* 11: 66–84.
12. Van Essen DC, Glasser MF, Dierker DL, Harwell J, Coalson T (2012) Parcellations and hemispheric asymmetries of human cerebral cortex analyzed on surface-based atlases. *Cereb Cortex* 22:2241–2262.
13. Sereno MI, et al. (1995) Borders of multiple visual areas in humans revealed by functional magnetic resonance imaging. *Science* 268:889–893.
14. Wandell BA, Winawer J (2011) Imaging retinotopic maps in the human brain. *Vision Res* 51:718–737.
15. Wang L, Mruczek RE, Arcaro MJ, Kastner S (2015) Probabilistic maps of visual topography in human cortex. *Cereb Cortex* 25:3911–3931.
16. Glasser MF, et al. (2016) A multi-modal parcellation of human cerebral cortex. *Nature* 536:171–178.
17. Carp J (2012) The secret lives of experiments: Methods reporting in the fMRI literature. *Neuroimage* 63:289–300.
18. Fischl B (2012) FreeSurfer. *Neuroimage* 62:774–781.
19. Glasser MF, et al.; WU-Minn HCP Consortium (2013) The minimal preprocessing pipelines for the Human Connectome Project. *Neuroimage* 80:105–124.
20. Robinson EC, et al. (2018) Multimodal surface matching with higher-order smoothness constraints. *Neuroimage* 167:453–465.
21. Robinson EC, et al. (2014) MSM: A new flexible framework for multimodal surface matching. *Neuroimage* 100:414–426.
22. Klein A, et al. (2009) Evaluation of 14 nonlinear deformation algorithms applied to human brain MRI registration. *Neuroimage* 46:786–802.
23. Fischl B, Sereno MI, Tootell RB, Dale AM (1999) High-resolution intersubject averaging and a coordinate system for the cortical surface. *Hum Brain Mapp* 8:272–284.
24. Van Essen DC (2005) A population-average, landmark- and surface-based (PALS) atlas of human cerebral cortex. *Neuroimage* 28:635–662.
25. Yeo BT, et al. (2010) Spherical demons: Fast diffeomorphic landmark-free surface registration. *IEEE Trans Med Imaging* 29:650–668.
26. Van Essen DC (2012) Cortical cartography and Caret software. *Neuroimage* 62: 757–764.
27. Hagler DJ, Jr, Saygin AP, Sereno MI (2006) Smoothing and cluster thresholding for cortical surface-based group analysis of fMRI data. *Neuroimage* 33:1093–1103.
28. Eickhoff SB, et al. (2005) A new SPM toolbox for combining probabilistic cytoarchitectonic maps and functional imaging data. *Neuroimage* 25:1325–1335.
29. Reuter M, et al. (2015) Head motion during MRI acquisition reduces gray matter volume and thickness estimates. *Neuroimage* 107:107–115.
30. Fischl B, et al. (2008) Cortical folding patterns and predicting cytoarchitecture. *Cereb Cortex* 18:1973–1980.
31. Glasser MF, Van Essen DC (2011) Mapping human cortical areas in vivo based on myelin content as revealed by T1- and T2-weighted MRI. *J Neurosci* 31:11597–11616.
32. Winkler AM, Ridgway GR, Webster MA, Smith SM, Nichols TE (2014) Permutation inference for the general linear model. *Neuroimage* 92:381–397.
33. Eklund A, Nichols TE, Knutsson H (2016) Cluster failure: Why fMRI inferences for spatial extent have inflated false-positive rates. *Proc Natl Acad Sci USA* 113:7900–7905.
34. Guntupalli JS, Feilong M, Haxby JV (2018) A computational model of shared fine-scale structure in the human connectome. *PLoS Comput Biol* 14:e1006120.
35. Sood MR, Sereno MI (2016) Areas activated during naturalistic reading comprehension overlap topological visual, auditory, and somatotomotor maps. *Hum Brain Mapp* 37:2784–2810.
36. Margulies DS, et al. (2016) Situating the default-mode network along a principal gradient of macroscale cortical organization. *Proc Natl Acad Sci USA* 113:12574–12579.
37. Zhang H, et al. (2007) High-dimensional spatial normalization of diffusion tensor images improves the detection of white matter differences: An example study using amyotrophic lateral sclerosis. *IEEE Trans Med Imaging* 26:1585–1597.
38. Zhang H, Yushkevich PA, Alexander DC, Gee JC (2006) Deformable registration of diffusion tensor MR images with explicit orientation optimization. *Med Image Anal* 10:764–785.
39. Zollei L, Stevens A, Huber K, Kakunoori S, Fischl B (2010) Improved tractography alignment using combined volumetric and surface registration. *NeuroImage* 51: 206–213.
40. Tong T, Aganj I, Ge T, Polimeni JR, Fischl B (2017) Functional density and edge maps: Characterizing functional architecture in individuals and improving cross-subject registration. *Neuroimage* 158:346–355.
41. Hacker CD, et al. (2013) Resting state network estimation in individual subjects. *Neuroimage* 82:616–633.
42. Wang D, et al. (2015) Parcellating cortical functional networks in individuals. *Nat Neurosci* 18:1853–1860.
43. Haxby JV, et al. (2011) A common, high-dimensional model of the representational space in human ventral temporal cortex. *Neuron* 72:404–416.

NEUROSCIENCE